

Photoemission studies of Ti_3SiC_2 and nanocrystalline-TiC/amorphous-SiC nanocomposite thin films

P. Eklund,^{1,*} C. Virojanadara,^{2,†} J. Emmerlich,¹ L. I. Johansson,² H. Högberg,¹ and L. Hultman¹

¹*Thin Film Physics Division, Department of Physics, Chemistry, and Biology, IFM, Linköping University, S-581 83 Linköping, Sweden*

²*Materials Physics Division, Department of Physics, Chemistry, and Biology, IFM, Linköping University, S-581 83 Linköping, Sweden*

(Received 15 February 2006; revised manuscript received 3 May 2006; published 17 July 2006)

Photoemission studies using synchrotron radiation have been performed on epitaxial $\text{Ti}_3\text{SiC}_2(0001)$ and compound nanocrystalline (nc-)TiC/amorphous (*a*-)SiC thin films deposited by magnetron sputtering. As-introduced samples were found to be covered by surface oxides, SiO_x and TiO_x . These oxides could be removed by *in-situ* annealing to $\sim 1000^\circ\text{C}$. For as-annealed $\text{Ti}_3\text{SiC}_2(0001)$, surface Si was observed and interpreted as originating from decomposition of Ti_3SiC_2 through Si out-diffusion. For nc-TiC/*a*-SiC annealed *in situ* to $\sim 1000^\circ\text{C}$, the surface instead exhibited a dominant contribution from graphitic carbon, also with the presence of Si, due to C and Si out-diffusion from the *a*-SiC compound or from grain boundaries.

DOI: [10.1103/PhysRevB.74.045417](https://doi.org/10.1103/PhysRevB.74.045417)

PACS number(s): 81.05.Je, 66.30.Pa, 68.60.-p, 81.07.Bc

I. INTRODUCTION

The ternary materials system Ti-Si-C has received much attention recently, for the exploration of its abundance of phases, such as the binaries TiC and SiC as well as the ternaries Ti_3SiC_2 and $\text{Ti}_5\text{Si}_3\text{C}_x$. Of particular interest to the present study are the structural and chemical relationships between the different phases, specifically TiC, Ti_3SiC_2 , and the two-phase nanocomposite consisting of nanocrystalline (nc-) TiC and amorphous (*a*-) SiC (abbreviated “nc-TiC/*a*-SiC”).

TiC is one of the interstitial transition-metal carbides,¹ which crystallize in a NaCl structure, where the metal atoms form layers with the carbon atoms placed in interstitial octahedral sites, thus forming edge-sharing octahedra. Some of the most notable properties of TiC, as well as the other transition-metal carbides, are high hardness, high melting point, and low thermal conductivity. While the presence of covalent bonding and the resulting high hardness makes it natural to consider TiC a ceramic, its electronic-transport mechanism is that of a metal, i.e., the electric charge is transported via conduction electrons.² The concentration of conduction electrons is, however, low; the density of states (DOS) at the Fermi level is ~ 0.08 states/eV cell.² A further important characteristic of the transition-metal carbides is their pronounced nonstoichiometry.³ The interstitial transition-metal carbides have a significant amount of carbon vacancies and a very large stability range. The carbon-to-metal ratio can assume values in the range of approximately 0.47–0.97 without any structural change.¹ This is usually written as TiC_x , where x is the carbon-to-metal ratio.

Ti_3SiC_2 is the most-studied member of the MAX-phase family. The MAX phases are a group of ternary layered compounds, whose composition is $\text{M}_{n+1}\text{AX}_n$ ($n=1-3$), where M is an early transition-metal (e.g., Ti, Zr), A is an A-group element (e.g., Si, Ge, Al), and X is C and/or N. Nowotny *et al.* originally synthesized these compounds in the 1960s,⁴ but the modern interest in these materials arose in the mid-1990s as a consequence of the work by Barsoum *et al.*,⁵ who sintered bulk samples of Ti_3SiC_2 and other MAX phases and

reported on their unique combination of metallic and ceramic properties. They are good electrical and thermal conductors, ductile and readily machinable, as well as damage tolerant and resistant to oxidation and thermal shock. Their remarkable properties stem from their nanolaminated crystal structure, which is hexagonal and highly anisotropic (the *c/a* ratio for Ti_3SiC_2 is ~ 5.8), with sheets of Si intercalated with TiC layers. Ti_3SiC_2 bears a close structural relationship to TiC, since they both consist of M_6X octahedral building blocks, or specifically Ti_6C . Just like in TiC, the Ti_6C octahedra in the MAX-phase structure share edges; however, the TiC blocks are interleaved with layers of pure A-elements (e.g., Si). The number of A-element layers thus inserted decides which MAX polytype is formed (M_2AX , M_3AX_2 , or M_4AX_3). In the Ti-Si-C system, the only thermodynamically stable MAX phase is Ti_3SiC_2 . Additionally, there is a metastable MAX phase, Ti_4SiC_3 , which has been synthesized in thin-film form.⁶

The large unit cell of the MAX phases requires a significant amount of thermal activation to form, i.e., a relatively high synthesis temperature, with typical values being 700–900 °C for sputtering⁶ and 1200–1400 °C for chemical vapor deposition (CVD) and bulk sintering.⁵ This is unacceptable for thin-film deposition on many metal substrates (e.g., Cu, Al, or steel), which are unable to withstand these temperatures. Consequently, significant scientific and technological efforts are being directed at understanding and employing Ti-Si-C thin films deposited by vapor processes at low temperature (typically from room temperature to 400 °C). In this kinetically restricted temperature range, however, the Ti-Si-C system does not tend to form MAX phases, but a nanocomposite consisting of one crystalline constituent, TiC_x , and one or more amorphous phases (denoted nc-TiC/*a*-SiC, as defined above).⁷ This nanocomposite has been shown to exhibit properties qualitatively similar to the MAX phases, notably a ductile mechanical behavior with hardness and elastic modulus values close to those of Ti_3SiC_2 , as well as low friction.^{7,8} Furthermore, nc-TiC/*a*-SiC exhibits metallic conductivity with a resistivity comparable to TiC_x .^{7,9} The combination of these mechanical and

electrical properties provides nc-TiC/*a*-SiC with potential for, e.g., electrical contact applications.

The structure, surface conditions, and bonding configuration of bulk Ti_3SiC_2 samples have been investigated by x-ray photoelectron spectroscopy (XPS) and x-ray or neutron diffraction.^{10,11} These diffraction methods have also been used to investigate the reaction paths during synthesis as well as decomposition of Ti_3SiC_2 .^{12,13} Synchrotron radiation has been employed to obtain high-resolution photoelectron spectra and reference data for the positions of the C $1s$, Si $2p$, and Ti $2p$ peaks obtained from sintered bulk Ti_3SiC_2 .¹⁴ The use of synchrotron radiation allowed the resolution of the spin-orbit splitting of the Si $2p$ peak. As for nc-TiC/*a*-SiC, numerous structural studies have been performed,⁷⁻⁹ but information on the surface conditions of as-deposited samples is relatively scarce.

In the present study, we perform photoemission investigations using synchrotron radiation on as-deposited as well as *in-situ* annealed Ti-Si-C samples (Ti_3SiC_2 and nc-TiC/*a*-SiC, with TiC_x investigated for comparison). The objective is twofold: to investigate the surface structure and composition of as-deposited samples and to investigate the effects of annealing. The annealing process serves two purposes, to remove any surface oxides present in the as-deposited state and to permit studies of decomposition processes. For Ti_3SiC_2 , the results can be summarized in that surface Si was observed for samples annealed to $\sim 1000^\circ\text{C}$. It originates from decomposition of Ti_3SiC_2 through Si out-diffusion due to the presence of an interface to the vacuum ambient. For annealed nc-TiC/*a*-SiC films, the surface instead exhibited graphitic carbon from C segregating to the phase boundaries of TiC and SiC in order to establish local (metastable) phase equilibria.

II. EXPERIMENTAL DETAILS

Photoemission measurements were performed on beam line I311 at the MAX synchrotron radiation laboratory in Lund, Sweden. This beam line is equipped with a modified SX-700 monochromator¹⁵ and an end station built up around a large hemispherical Scienta electron analyzer,¹⁶ which operates under ultrahigh vacuum (UHV) conditions, at a base pressure of about 1×10^{-10} torr. The electron analyzer accepts a cone of angular width $\pm 8^\circ$. A total-energy resolution, determined by the operating parameters used, of ≤ 20 meV at a photon energy of 240 eV, of ≤ 100 meV at 330 eV, and of ≤ 300 meV at 600 eV was selected in the high-resolution studies of the Si $2p$, C $1s$, O $1s$, and Ti $2p$ core levels reported below.

The investigations were carried out on thin-film samples of epitaxial $\text{Ti}_3\text{SiC}_2(0001)$, nanocomposite nc-TiC/*a*-SiC, and epitaxial TiC(111). The surface cleanliness was checked by monitoring the core levels of likely contaminants and the surface order was verified by low energy electron diffraction (LEED). The oxide thickness on as-introduced samples was determined using a layer attenuation model.¹⁷ The samples were ohmically heated *in situ* and the temperature was monitored using an IR pyrometer assuming an emissivity of 0.3, equal to that of TiC. For the clean surfaces (without oxide),

the binding energies were determined relative to the Fermi edge of a Ta foil on the sample holder. For the as-introduced samples, the binding energies were referenced to the bulk C $1s$ and Si $2p$ levels of samples in order to correct for changes in the band bending and for possible charging effects.

Ti_3SiC_2 and TiC thin-film samples were synthesized using dc magnetron sputtering from elemental Ti, Si, and C targets in an ultrahigh vacuum onto $\text{Al}_2\text{O}_3(0001)$ substrates. A Ti_3SiC_2 target was employed to deposit nc-TiC/*a*-SiC onto a Si (001) substrate. The substrate temperature was 850°C for Ti_3SiC_2 , 300°C for a nc-TiC/*a*-SiC sample, and 450°C for the TiC samples. The synthesis process is described in detail elsewhere.^{7,18} The structure of the resulting samples was determined by a combination of x-ray diffraction (XRD) and transmission electron microscopy (TEM).^{7,18}

III. RESULTS AND DISCUSSION

A. General observations

For the single-crystal $\text{Ti}_3\text{SiC}_2(0001)$ and nanocomposite nc-TiC/*a*-SiC samples, only Ti, Si, and C core levels were observed from the survey spectra collected after annealing to $\sim 1000^\circ\text{C}$. No oxygen could be observed after annealing. The TiC(111), however, showed an additional peak from O $1s$ even after annealing to 1100°C .

All as-introduced samples exhibited peaks originating from surface oxides corresponding to Si-O, Ti-O, and C-O bonding, and with a strong O $1s$ signal in the survey spectra. The oxide thickness was determined to 25 \AA for the $\text{Ti}_3\text{SiC}_2(0001)$ sample, $35\text{--}40 \text{ \AA}$ for the nc-TiC/*a*-SiC sample, and 30 \AA for the TiC(111) sample. The surface oxides will be further discussed in Sec. III E.

B. Ti_3SiC_2

Si $2p$ spectra from a single-crystal, epitaxial Ti_3SiC_2 film recorded before and after annealing using a photon energy of 240 eV are shown in Figs. 1(a) and 1(b), respectively. The Si $2p$ spectrum from the as-introduced sample shows a dominant contribution from surface oxides. No LEED pattern could be observed. The surface oxide was removed by ~ 3 min of *in-situ* annealing at 1000°C . The surface was then well ordered and exhibited a 1×1 LEED pattern as shown in the inset in Fig. 1(b). The components obtained after fitting^{19,20} are also shown in Fig. 1. The Si $2p$ spectrum after annealing consists of three components. The middle component has a binding energy similar to that observed for pure silicon (absolute value 99.2 eV),^{10,21} while the two others exhibit shifts of $+0.9(0.07) \text{ eV}$ and $-0.4(0.05) \text{ eV}$, respectively, where the values specified in brackets are the standard deviations of the determined values. The weak component, with a shift of $+0.9 \text{ eV}$, corresponds to the binding energy of Si $2p$ in bulk SiC.^{10,22} The dominant component, with a shift of -0.4 eV , corresponds to Si atoms in Ti_3SiC_2 .¹⁴

Scanning the photon energies from 140 to 600 eV (i.e., varying the surface sensitivity) resulted in a variation in the relative intensity ratio of the three components of the Si $2p$ spectrum. The component corresponding to Si-Si bonding

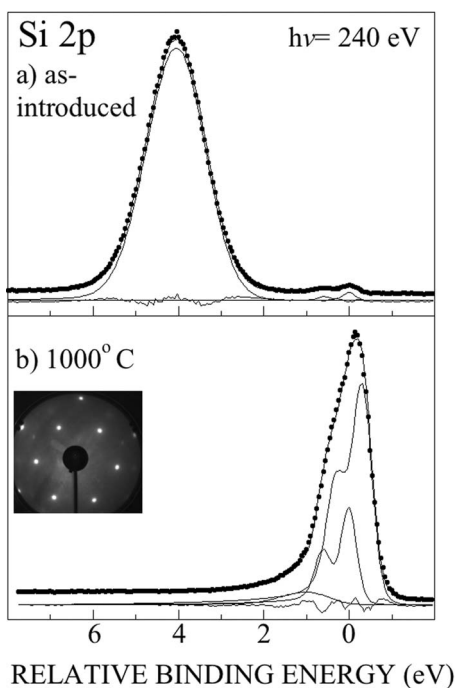


FIG. 1. Si $2p$ spectra recorded using a photon energy of 240 eV from the $\text{Ti}_3\text{SiC}_2(0001)$ single-crystal sample, (a) as-introduced and (b) after annealing at 1000 °C for 3 min., respectively. The solid curves show the fitted components and results obtained. The 1×1 LEED pattern recorded from the annealed surface at 180 eV is shown in the inset. The residuals of the fits are also shown.

exhibited a higher relative intensity for lower photon energies; i.e., this component is surface related, while the two peaks originating from Si atoms in Ti_3SiC_2 and from Si-C bonding exhibited lower intensities for lower photon energies, i.e., these components are bulk related. These results suggest that a thin Si layer is located on top of the Ti_3SiC_2 , with the presence of a small amount of SiC. This can be interpreted in two ways. It could be due to Si termination of the Ti_3SiC_2 surface, i.e., that the Ti_3SiC_2 thin film is terminated by its A-element layers in equilibrium with vacuum. If this were the case, however, there is no reason why we should observe Si-C bonding, since this bonding configuration is not present in Ti_3SiC_2 . The more likely interpretation is that we observe the start of a Ti_3SiC_2 decomposition process through Si out-diffusion. This decomposition process is believed to occur according to a model proposed by Barsoum,⁵ where the Ti_3C_2 layers between Si sheets in Ti_3SiC_2 represent $\text{TiC}(111)$ planes. The Ti_3C_2 layers are twinned to each other separated by the Si layer acting as a mirror plane. De-twinning to TiC occurs upon removal of the Si plane and rotation of the Ti_3C_2 layer, which means that, at a temperature of ~ 1000 °C, Si starts to diffuse out along the basal planes of the Ti_3SiC_2 structure, followed by rotation of the Ti_3C_2 structural units to form TiC. This interpretation corroborates well with what has been observed in XRD *in-situ*-annealing experiments on thin-film epitaxial Ti_3SiC_2 , where decomposition into TiC and gaseous Si has been observed to occur between 1100 °C and 1200 °C.²³ As a small amount of graphitic C is present also after annealing (see below), some of the Si diffusing out of the Ti_3SiC_2 structure

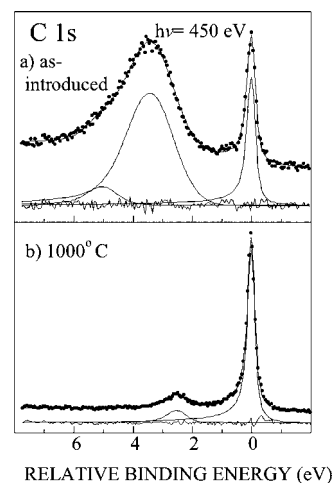


FIG. 2. C $1s$ spectra recorded using a photon energy of 450 eV from the $\text{Ti}_3\text{SiC}_2(0001)$ sample, (a) as-introduced and (b) after annealing at 1000 °C for 3 min., respectively. The results from curve fits, the components used, and the residuals of the fits are also shown.

may bond to C, which would explain our observation of Si-C bonding in annealed films. The actual temperatures are considerably lower than the temperature required for decomposition of bulk Ti_3SiC_2 .⁵ The consensus in the literature is that dense, sintered Ti_3SiC_2 is effectively thermally stable up to at least 1700 °C,^{5,13} but possibly up to above 2300 °C.²⁴ There is thus an apparent difference between epitaxial thin-film samples and bulk samples with respect to the decomposition findings for Ti_3SiC_2 . The obvious factor in resolving the contradiction lies in that the diffusion length scales and the sensitivity of the analysis methods are different in the actual studies. More importantly, with the presence of an interface to ambient the chemical potentials for the elements are reduced. In the presence of oxygen, surface oxides will thus form that can act as diffusion barriers against further decomposition. In the present thin film study, the UHV conditions presented effectively no oxidizing environment. Instead, Si—as a relatively weakly bonded atom and the fastest diffusing species compared to Ti and C—tended to segregate to the surface at 1000 °C. With the very short diffusion length scales required for the surface sensitivity of our experiments on the thin-film epitaxial Ti_3SiC_2 samples, it is thus not surprising that we could find the onset temperature for MAX phase decomposition. It should further be noted that the decomposition temperature of bulk Ti_3SiC_2 is lower than stated above if a chemical driving force is provided for increasing the Si segregation. This has been shown to occur through carburization²⁵ or immersion in molten cryolite.²⁶ In our case the driving force may be provided by the presence of a surface/vacuum interface.

Figures 2(a) and 2(b) show the C $1s$ spectra from the $\text{Ti}_3\text{SiC}_2(0001)$ sample in as-introduced and annealed (1000 °C for 3 min) states, respectively. The components obtained after fitting²⁷ are also shown. Binding energies are specified relative to the peak corresponding to the component originating from C in the Ti_3SiC_2 phase (absolute value 282.1 eV). In addition to this peak, a broad feature is ob-

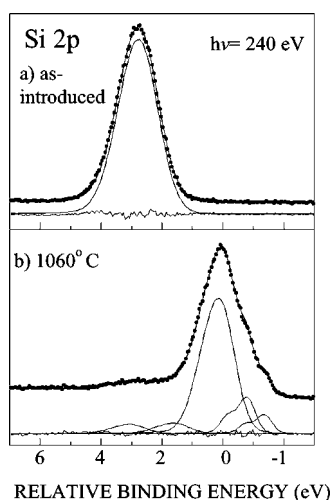


FIG. 3. Si $2p$ spectra recorded using a photon energy of 240 eV from the nc-TiC/*a*-SiC nanocomposite sample, (a) as-introduced and (b) after annealing at 1060 °C for 3 min., respectively. The results from curve fits, the components used, and the residuals of the fits are also shown.

served in the spectrum obtained from the as-introduced sample. Modeling of this feature requires two components, with relative binding energies of +5.1 (0.10) eV and +3.4 (0.06) eV, respectively. We interpret these components as originating from hydrocarbon contamination on the as-introduced surface. After annealing, only one component (apart from the peak originating from C in Ti_3SiC_2) is observed, with a shift of +2.5 (0.05) eV. This corresponds to graphitic C.²⁸

While the hydrocarbon contamination desorbs during annealing, the C-C bonding observed after annealing indicates that graphitic carbon either was formed during the annealing process, or was present on the as-introduced sample and remained on the surface throughout the annealing experiment. A comparison with what is known for TiC can shed light on the origin of this surface C. The fact that TiC adopts a NaCl structure means that the 111 surface is ideally terminated by either Ti or C. In annealing studies where TiC is in equilibrium with vacuum, TiC(111) is always observed to be Ti terminated, as a consequence of the different evaporation rates for Ti and C atoms.^{29,30} Given the isomorphism of TiC(111) and $\text{Ti}_3\text{SiC}_2(0001)$ surfaces and the Ti predominance in the latter phase, it is reasonable to assume that $\text{Ti}_3\text{SiC}_2(0001)$ is not naturally C terminated, and consequently that the observed surface C is likely to be of foreign origin.

C. nc-TiC/*a*-SiC

Si $2p$ spectra recorded from nc-TiC/*a*-SiC nanocomposite samples in as-introduced and annealed states are shown in Figs. 3(a) and 3(b), respectively, together with results obtained after fitting. For the as-introduced sample, only a surface oxide was detected, very similar to that observed for the $\text{Ti}_3\text{SiC}_2(0001)$ sample. After annealing to 1060 °C, the oxide signal was strongly reduced and additional components

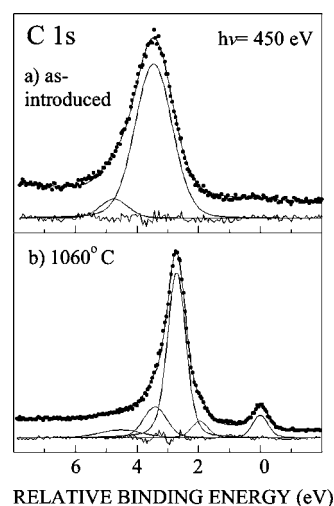


FIG. 4. C $1s$ spectra recorded using a photon energy of 450 eV from the nc-TiC/*a*-SiC sample, (a) as-introduced and (b) after annealing at 1060 °C for 3 min., respectively. The results from curve fits, the components used, and the residuals of the fits are also shown.

appeared. The component with the highest intensity corresponds to Si-C bonding; its binding energy (100.3 eV) is similar to that of bulk SiC.²² This component is assigned the relative binding energy of zero. At lower binding energies, two components with shifts of $-0.8(0.07)$ eV and $-1.3(0.05)$ eV are observed. Similarly, on the higher binding energy side, two components with shifts of $+3.0(0.11)$ eV and $+1.6(0.11)$ eV are observed. These four components are surface related since their relative intensities decreased when higher photon energies were selected. The origin of the component at -0.8 eV is most likely Si-Si bonds,²¹ while the component at -1.3 eV is more ambiguous. The shift, however, agrees with that obtained above for the epitaxial Ti_3SiC_2 film, and may therefore be an indication that a small amount of Ti_3SiC_2 has formed upon annealing. It could also be due to silicide formation; the Si $2p$ peak position for TiSi_2 (or TiSi_x) is very close to that of Ti_3SiC_2 .¹¹ It should be pointed out that XRD and high-resolution TEM of the as-deposited nc-TiC/*a*-SiC samples⁷ showed no Ti_3SiC_2 or silicides.

The components located at the higher binding energy side, with shifts of +3.0 and +1.6 eV, can be interpreted as two types of oxidation states present on the surface, Si^{+4} (SiO_2) and Si^{+2} , respectively.³¹ The presence of the Si^{+2} oxidation state on the surface is an indication that the surface is carbon rich, since this oxidation state tends to be present on C terminated SiC surfaces.³² This interpretation is further supported by the C $1s$ spectra discussed below.

The C $1s$ spectrum from the as-introduced nc-TiC/*a*-SiC sample shows only contributions from surface hydrocarbon contamination, as illustrated in Fig. 4(a), similar to what was observed for the Ti_3SiC_2 sample [Fig. 2(a)]. After annealing at 1060 °C for 3 min., the main component in the C $1s$ spectrum is a graphitelike peak, as shown in Fig. 4(b). A weaker component originating from the C-Ti bonding in TiC appears at 2.7 (0.01) eV lower binding energy than the

dominant graphitelike peak. We note that when lower photon energies were selected, the relative intensity of the graphite-like peak was high, and that its relative intensity was lower when higher photon energy (600 eV) was used. Consequently, we conclude that the graphite is predominantly present on the surface. The graphitelike component is much more pronounced in this sample than in the single-crystal Ti₃SiC₂ sample. Partially, this is due to surface carbon present already in the as-deposited state (i.e., after synthesis but before exposure to atmosphere), as has been observed in preliminary *in-situ* XPS measurements.³³ Additionally, three weaker components have to be introduced to satisfactorily fit recorded data, with shifts of +4.8 (0.23), +3.5 (0.16), and +1.9 (0.11) eV relative to the C 1s C-Ti peak. These additional components are suggested to originate from residual surface hydrocarbon contamination after heating,^{34,35} but particularly the highest-energy component is weak and could be an artifact.

Based on these results, we propose that during annealing of nc-TiC/*a*-SiC, C and Si diffuse out from the composite material, resulting in the presence of surface Si-Si and C-C bonds. This is in contrast to Ti₃SiC₂, where the decomposition process occurs exclusively through Si out diffusion, while C is tightly bonded in the Ti₆C octahedral structural units. In the TiC(111) film (see Sec. III D), no surface C was observed, since C is even more tightly bonded than in Ti₃SiC₂. Consequently, it can be concluded that the surface C and Si observed in the case of annealed nc-TiC/*a*-SiC originates from the *a*-SiC phase or from grain boundaries, while it should be noted that some surface C is present already in the as-deposited state before exposure to atmosphere.

D. Comparison with TiC_x

For comparison, photoemission data were recorded from a single-crystal TiC_x(111) thin film. C 1s spectra collected from the as-introduced TiC sample and after annealing at 1100 °C for 3 min are shown in Fig. 5. The hydrocarbon contamination present on the as-introduced surface, as seen in Fig. 5(a), is no longer present after annealing [Fig. 5(b)], as only one symmetric C 1s peak is observed. Unlike the epitaxial Ti₃SiC₂ film and in particular the nc-TiC/*a*-SiC film, no graphitic C was present on the surface after annealing. This lends support to our proposed model for the elemental segregations in nc-TiC/*a*-SiC: as stated in Sec. III C, the graphitic surface C observed after annealing of nc-TiC/*a*-SiC most likely does not originate from the nc-TiC phase.

After annealing of the TiC film, a distinct 1 × 1 TiC(111) LEED pattern (not shown) was observed, although an O 1s signal could be observed by photoemission. Presence of oxygen on the surface was also revealed in recorded Ti 2p spectra (Fig. 6), as indicated by the shoulder located at the high binding energy side of the Ti 2p doublet peak. When comparing the Ti 2p peaks for TiC, Ti₃SiC₂, and nc-TiC/*a*-SiC, we note that the shoulder is most pronounced for the TiC film, smaller for the nc-TiC/*a*-SiC film, and essentially not present for the Ti₃SiC₂ film. This can be interpreted as the presence of TiO_x on the surfaces of the TiC and nc-TiC/

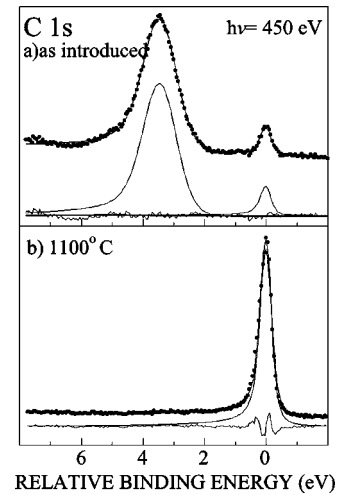


FIG. 5. C 1s spectra recorded using a photon energy of 450 eV from the TiC(111) sample, (a) as-introduced and (b) after annealing at 1100 °C for 3 min., respectively. The results from curve fits, the components used, and the residuals of the fits are also shown.

a-SiC films, but any O in a solid solution with the TiC structure³⁶ is also expected to contribute to the shoulder.

E. Surface oxides

O 1s spectra collected at a photon energy of 600 eV from the three different as-introduced films are shown in Fig. 7. Two components are clearly visible in the TiC and nc-TiC/*a*-SiC spectra. When fitting, the low-binding-energy component was found to be present also in the spectrum from Ti₃SiC₂(0001), although with considerably lower relative intensity. The separation between the two components is found to increase somewhat when going from nc-TiC/*a*-SiC to Ti₃SiC₂ to TiC, from +1.4 to +1.9 eV. The component located at lower binding energy probably corresponds to TiO_x present on the surface, as discussed above. The component at higher binding energy may originate from the mixture between Si-O-C bonding in a different atomic ratio for the nc-TiC/*a*-SiC and Ti₃SiC₂ films and Ti-O-C bonding for

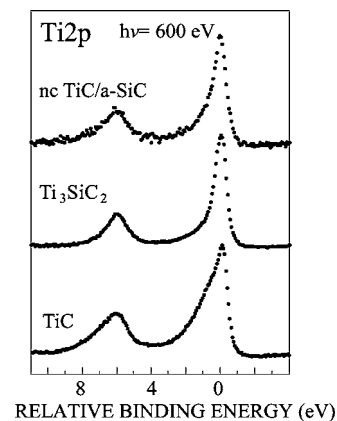


FIG. 6. Ti 2p spectra collected from the TiC(111), Ti₃SiC₂(0001), and nc-TiC/*a*-SiC nanocomposite samples, respectively. A photon energy of 600 eV was used.

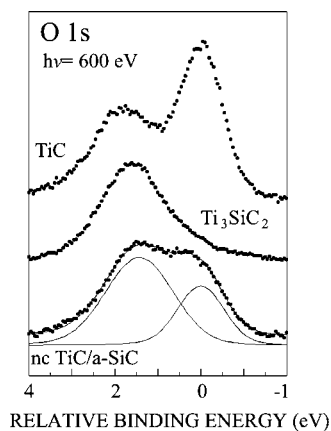


FIG. 7. O $1s$ core level spectra collected from the nc-TiC/ a -SiC nanocomposite, $Ti_3SiC_2(0001)$, and TiC(111) samples, respectively. A photon energy of 600 eV was used. The results from curve fits and the components used are also shown.

the TiC film. In the latter case, this interpretation is supported by the fact that O has a solid solubility in the TiC structure;³⁶ the two peaks observed in the O $1s$ spectrum from TiC can therefore be seen as originating from TiO_x and TiC_xO_y . The observation of two oxides (TiO_x and SiO_x) present on the nc-TiC/ a -SiC is consistent with what has been observed previously.⁷ Note that the Si $2p$ peak from the annealed nc-TiC/ a -SiC film exhibited two types of oxidation states present on the surface, Si^{+4} and Si^{+2} , where the presence of the latter is an indication that the surface is carbon rich. The TiO_x peak in the Ti_3SiC_2 sample is, however, much smaller, i.e., the oxide on the Ti_3SiC_2 sample is predominantly SiO_x . Given the larger separation between the TiO_x and SiO_x peaks for the Ti_3SiC_2 sample than for the nc-TiC/ a -SiC sample, it is probable that the SiO_x contains C, in other words a mixture of Si-O-C bonding.³²

IV. CONCLUSIONS

We have performed photoemission studies using synchrotron radiation of as-introduced and annealed thin films of

epitaxial $Ti_3SiC_2(0001)$ and nanocomposite nc-TiC/ a -SiC. As-introduced samples exhibited peaks originating from surface oxides, SiO_x and TiO_x . The oxide thickness was determined to 25 Å for $Ti_3SiC_2(0001)$ and 35–40 Å for the nc-TiC/ a -SiC sample. The oxides were removed by annealing to ~ 1000 °C.

On annealed $Ti_3SiC_2(0001)$, surface Si was observed and interpreted as originating from decomposition of Ti_3SiC_2 through Si out-diffusion. The present annealing temperatures are considerably lower than the temperature (≥ 1700 °C) reported for effective decomposition of bulk Ti_3SiC_2 . The difference in observed decomposition temperature for the two structures is a consequence of the type of experiment and measurement sensitivity employed in the respective studies. We find that the MAX phase Ti_3SiC_2 decomposes as Si diffuses out of the material due to the chemical driving force towards the ambient (i.e., a difference in chemical potential) at a free surface for which we have atomic-layer sensitivity. In consequence, we propose that also bulk samples may exhibit initial decomposition with respect to TiC formation at grain boundaries, as these may serve as sinks for Si just like the free surface.

For annealed nc-TiC/ a -SiC, the surface instead exhibited a dominant contribution from graphitic carbon, also with the presence of some free Si. This was attributed in part to surface C present in the as-deposited state, but more significantly to the out-diffusion of C (and Si) from the amorphous SiC phase or from grain boundaries. Effectively, a three-phase nanocomposite consisting of TiC, SiC, and graphitic C was formed.

ACKNOWLEDGMENTS

We acknowledge The Swedish Agency for Innovation Systems (VINNOVA), The Swedish Research Council (VR), the Swedish Foundation for Strategic Research (SSF), Impact Coatings AB, ABB AB, and Kanthal AB for support.

*Corresponding author. E-mail address: perek@ifm.liu.se

†Present address: MPI für Festkörperforschung, Grenzflächenanalytik, Heisenbergstrasse 1, D-705 69 Stuttgart, Germany.

¹W. S. Williams, *Prog. Solid State Chem.* **6**, 57 (1971).

²W. S. Williams, *Mater. Sci. Eng., A* **105/106**, 1 (1988).

³H. O. Pierson, *Handbook of Refractory Carbides and Nitrides* (Noyes Publications, Westwood, 1996).

⁴H. Nowotny, *Prog. Solid State Chem.* **2**, 27 (1970).

⁵M. W. Barsoum, *Prog. Solid State Chem.* **28**, 201 (2000).

⁶J.-P. Palmquist, S. Li, P. O. Å. Persson, J. Emmerlich, O. Wilhelmsson, H. Högberg, M. I. Katsnelson, B. Johansson, R. Ahuja, O. Eriksson, L. Hultman, and U. Jansson, *Phys. Rev. B* **70**, 165401 (2004).

⁷P. Eklund, J. Emmerlich, H. Högberg, O. Wilhelmsson, P. Isberg, J. Birch, P. O. Å. Persson, U. Jansson, and L. Hultman, *J. Vac. Sci. Technol. B* **23**, 2486 (2005).

⁸A. R. Phani, J. E. Krzanowski, and J. J. Nainaparampil, *J. Vac. Sci. Technol. A* **19**(5), 2252 (2001).

⁹S. H. Koutzaki, J. E. Krzanowski, and J. J. Nainaparampil, *J. Vac. Sci. Technol. A* **19**(4), 1912 (2001).

¹⁰E. H. Kisi, J. A. A. Crossley, S. Myhra, and M. W. Barsoum, *J. Phys. Chem. Solids* **59**, 1437 (1998).

¹¹D. P. Riley, J. J. O'Connor, P. Dastoor, N. Brack, and P. J. Pigram, *J. Phys. D* **35**, 1603 (2002).

¹²E. Wu, E. H. Kisi, S. J. Kennedy, and A. J. Studer, *J. Am. Ceram. Soc.* **84**, 2281 (2001).

¹³R. Radakrishnan, J. J. Williams, and M. Akinc, *J. Alloys Compd.* **285**, 85 (1999).

¹⁴S. E. Stoltz, H. I. Starnberg, and M. W. Barsoum, *J. Phys. Chem. Solids* **64**, 2321 (2003).

¹⁵R. Nyholm, S. Svensson, J. Nordgren, and S. A. Flodström, *Nucl. Instrum. Methods Phys. Res. A* **246**, 267 (1986).

- ¹⁶J. N. Andersen, O. Björnholm, A. Sandell, R. Nyholm, J. Forsell, L. Thånell, A. Nilsson, and N. Mårtensson, *Synchrotron Radiat. News* **4**, 15 (1991).
- ¹⁷L. I. Johansson, C. Virojanadara, Th. Eickhoff, and W. Drube, *Surf. Sci.* **529**, 515 (2003).
- ¹⁸J. Emmerlich, J.-P. Palmquist, H. Högberg, J. M. Molina-Aldareguia, Zs. Czigány, Sz. Sasvári, P. O. Å. Persson, U. Jansson, and L. Hultman, *J. Appl. Phys.* **96**, 4817 (2004).
- ¹⁹P. H. Mahowald, D. J. Friedman, G. P. Carey, K. A. Bertness, and J. J. Yeah, *J. Vac. Sci. Technol. A* **5**, 2982 (1987).
- ²⁰The parameters selected for the Si *2p* levels were a spin-orbit splitting of 0.61 eV, a branching ratio of 0.50, a Lorentzian width of 0.07 and asymmetry parameter values of 0.07–0.10. All of these were fixed parameters for each sample. Variable parameters were the peak energies, the relative intensities, and the Gaussian widths. Best fits were obtained for Gaussian widths of 1.0, 0.5, and 0.4 eV for the higher shift, the lower shift and the reference peak, respectively. Details about fitting procedures and parameters can be found in Ref. 19.
- ²¹G. Hollinger and F. J. Himpsel, *J. Vac. Sci. Technol. A* **1**, 640 (1983).
- ²²C. Virojanadara and L. I. Johansson, *Phys. Rev. B* **71**, 195335 (2005).
- ²³J. Emmerlich, D. Music, P. Eklund, O. Wilhelmsson, U. Jansson, J. Schneider, H. Högberg, and L. Hultman (unpublished).
- ²⁴Y. Du, J. C. Schuster, H. Seifert, and F. Aldinger, *J. Am. Ceram. Soc.* **83**, 197 (2000).
- ²⁵T. El-Raghy and M. W. Barsoum, *J. Appl. Phys.* **83**, 112 (1998).
- ²⁶M. W. Barsoum, T. El-Raghy, L. Farber, M. Amer, R. Cristini, and A. Adams, *J. Electrochem. Soc.* **146**, 3919 (1999).
- ²⁷The parameters selected for the C *1s* level were a Lorentzian width of 0.18 and asymmetry parameter values of 0.07–0.10. For as-introduced samples, best fits were obtained for a Gaussian width of 0.2, 1.7, and 1.1 eV for the main peak and the shifted components, respectively. After annealing, the peak was best modeled using a Gaussian width of 0.15 and 0.7 eV, respectively, for the main peak and the shifted component.
- ²⁸S. Hirono, S. Umemura, M. Tomita, and R. Kaneko, *Appl. Phys. Lett.* **80**, 425 (2002).
- ²⁹C. Oshima, M. Aono, S. Zaima, Y. Shibata, and S. Kawai, *J. Less-Common Met.* **82**, 69 (1981).
- ³⁰K. E. Tan, M. W. Finnis, A. P. Horsfield, and A. P. Sutton, *Surf. Sci.* **348**, 49 (1996).
- ³¹J. H. Oh, H. W. Yeom, Y. Hagimoto, K. Ono, M. Oshima, N. Hirashita, M. Nywa, A. Toriumi, and A. Kakizaki, *Phys. Rev. B* **63**, 205310 (2001).
- ³²C. Virojanadara and L. I. Johansson, *Phys. Rev. B* **68**, 125314 (2003).
- ³³P. Eklund, J. Emmerlich, R. Haasch, I. Petrov, H. Högberg, and L. Hultman (unpublished).
- ³⁴F. S. Tautz, S. Sloboshanin, U. Starke, and J. A. Schaefer, *Surf. Sci.* **470**, L25 (2000).
- ³⁵L. I. Johansson, F. Owman, and P. Mårtensson, *Phys. Rev. B* **53**, 13793 (1996).
- ³⁶D. Gozzi, M. Montozzi, and P. L. Cignini, *Solid State Ionics* **123**, 1 (1999).